Advances in Nano Research, *Vol. 7 No. 3 (2019) 169-180*
DOI: https://doi.org/10.12989/anr.2019.7.3.169

Plasmonic effects and size relation of gold-platinum alloy nanoparticles

Muhammad Jawad [1], Shazia Ali [1], Amir Waseem [2], Faiz Rabbani [3], Bilal Ahmad Zafar Amin [4], Muhammad Bilal [4] and Ahson J. Shaikh [*1]

[1] *Department of Chemistry, COMSATS University Islamabad – Abbottabad Campus, Abbottabad-22060, KPK, Pakistan*
[2] *Department of Chemistry, Quaid-i-Azam University, Islamabad-45320, Pakistan*
[3] *Department of Environmental Sciences, COMSATS University Islamabad – Vehari Campus, Vehari, Pakistan*
[4] *Department of Environmental Sciences, COMSATS University Islamabad – Abbottabad Campus, Abbottabad-22060, KPK, Pakistan*

(*Received December 20, 2018, Revised March 29, 2019, Accepted April 21, 2019*)

Abstract. Plasmonic effects of gold and platinum alloy nanoparticles (Au-Pt NPs) and their comparison to size was studied. Various factors including ratios of gold and platinum salt, temperature, pH and time of addition of reducing agent were studied for their effect on particle size. The size of gold and platinum alloy nanoparticles increases with increasing concentration of Pt NPs. Temperature dependent synthesis of gold and platinum alloy nanoparticles shows decrease in size at higher temperature while at lower temperature agglomeration occurs. For pH dependent synthesis of Au-Pt nanoparticles, size was found to be increased by increase in pH from 4 to 10. Increasing the time of addition of reducing agent for synthesis of pure and gold-platinum alloy nanoparticles shows gradual increase in size as well as increase in heterogeneity of nanoparticles. The size and elemental analysis of Au-Pt nanoparticles were characterized by UV-Vis spectroscopy, XRD, SEM and EDX techniques.

Keywords: gold nanoparticles; platinum nanoparticles; bimetallic nanoparticles, alloy nanoparticles; plasmonic effects; Au-Pt

1. Introduction

Alloying of metals is an approach to develop new materials having different structural, chemical and physical properties than pure metals (Anicetus Muche 2010). Alloy nanoparticles or nano alloys are being considered as fascinating materials which can be applied to various applications including electronics, engineering and catalysis because of the rich diversity of composition, structures and properties of different metals (Ferrando *et al*. 2008). Gold platinum alloy nanoparticles have massive interest for important catalytic reactions including CO-oxidation, hydrogen-evolution, electrocatalytic oxygen reduction, electrooxidation and hydrogenation (Calvo 2013) etc.

Synthetic methods for controlling size (Mathis *et al*. 2016), shape (Choi *et al*. 2014), metallic content and tuning of optical properties for few types of alloy nanoparticles are known (Huang *et al*. 2007). Studies show control in size of alloy nanoparticles by changing reactions conditions such as increase in particle size by increasing temperature for Pd–Co/C alloys (Wang *et al*. 2007) and FePt (Chen *et al*. 2004). Similarly, size can be controlled by changing the pH in reaction mixture, e.g. an average particle size of 1-4 nm of Ti/Ni bimetallic nanoparticles can be modified by changing pH from 4 – 7 (Schabes-Retchkiman *et al*. 2006). In case of Pt-Ag/c average particle size was increased by increasing pH (Hwang *et al*. 2008). Furthermore, it is well known that size can be controlled by varying the composition of the precursor salt ratio e.g. Au-Ag alloy nanoparticles (Shaikh *et al*. 2018). Similarly, particle size of Cu-Ag alloy nanoparticles were found to be in 20-25 nm range by changing the composition of Cu and Ag (Valodkar *et al*. 2011).

Dong *et al* have developed a method for synthesis of Au-Pt alloy nanoparticles by varying molar ratios of gold and platinum by using co-reduction of chloroplatinic and chloroauric acid by using hydrazine. They have made Au-Pt nanoalloys having sizes of 3-5 nm (Wu *et al*. 2001). Sun *et al*. (2016) have proposed a one-step method for formation of Au-Pt alloy nanoparticles in aqueous solution having average particle size of 60 nm. He *et al*. (2017) have made Au-Pt alloy nanoparticles by varying composition through co-reduction of gold and platinic acid in aqueous solution having average particle sizes of 20 nm – 40 nm.

To the best of our knowledge, there is no proper method present for controlling the size of Au-Pt alloy nanoparticles using any simple-chemical method. In this article we have proposed a methodology to synthesize Au-Pt alloy nanoparticles using low cost and mild reducing agent i.e. trisodium citrate. Different factors such as time of addition of reducing agent, ratio of gold and platinum salts, temperature and pH have been studied and reported for their effects on particle size and plasmonic effects.

2. Materials and methods

99.99% $H_2PtCl_6 \cdot 6H_2O$ hexacholoroplatinic acid was purchased from BDH chemicals Ltd, China. 1.0 g of

*Corresponding author, Ph.D.,
E-mail: ahsonjabbar@hotmail.com; ahson@cuiatd.edu.pk

ISSN: 2287-237X (Print), 2287-2388 (Online)

$H_2PtCl_6 \cdot 6H_2O$ was dissolved in 193 mL of distilled water in order to prepare 0.01 M stock solution. 99.99% $HAuCl_4.4H_2O$ hydrogen tetrachloroaurate (III) was purchased from Guangdong Guanghua chemical factory Co. Ltd, Shantou, Guangdong, China. 1.0 g of $HAuCl_4.4H_2O$ was dissolved in 243 mL of distilled water in order to prepare a 0.01 M stock solution. Both prepared solutions were safely stored in screw bottles which were wrapped in a aluminum foil and were placed in a dark cabinet at room temperature for future use. Trisodium citrate ($C_6H_5Na_3O_7 \cdot 2H_2O$; purchased from Fluka) was used to prepare 1% trisodium citrate by dissolving 0.5 g in 50 mL of distilled water using measuring cylinder which was used as stabilizer as well as reducing agent.

2.1 Synthesis of pure platinum nanoparticles

The citrate capped platinum nanoparticles were prepared as described by Henglein and co-workers (Henglein *et al.* 1995). To prepare 0.0003 M solution, 3 mL of 0.01 M $H_2PtCl_6 \cdot 6H_2O$ was dissolved in 97 mL distilled water and heated to boiling at 100°C along with continuous stirring in a 250 mL conical flask. 5 mL of 1% trisodium citrate solution was heated and quickly added to boiling $H_2PtCl_6 \cdot 6H_2O$ solution. The color of platinum salt solution started to change from yellowish to transparent and finally to light brown which indicated the formation of Pt NPs. The resulting solution was allowed to boil for about an hour and then cooled down at room temperature.

2.2 Synthesis of pure gold nanoparticles

Au NPs were synthesized by the Turkevich method according to the method given in the literature (Kimling *et al*. 2006). To prepare 100 mL solution of Au NPs, 7.1 mL of 0.01M solution of $AuCl_3.HCl.4H_2O$ was dissolved in 88 mL of distilled water using conical flask. The solution temperature was kept at 100°C along with continuous stirring on magnetic stirrer. 5 mL solution of 1% trisodium citrate was heated and then added quickly to boiling solution of $AuCl_3.HCl.4H_2O$. After the addition of reducing agent, the yellowish color of $AuCl_3$ solution becomes transparent and finally changes to wine red color which indicates the formation of Au NPs. After color changing the solution was further heated for 15 minutes. Heating was stopped after the preparation of Au NPs and then allowed to cool at room temperature. During boiling the loss was compensated by the addition of distilled water and the solution level was made up to 100 mL.

2.3 Synthesis of gold and platinum alloy nanoparticles

Alloy nanoparticles (1:1 ratio) were prepared by a reported method (Essinger-Hileman *et al*. 2011). 3.5 mL of 0.01M $H_2PtCl_6.H_2O$ and 3.5 mL of 0.01 M $AuCl_3.HCl.4H_2O$ were dissolved in 88 mL of distilled water in a conical flask. Heating was done to boil the solution at 100°C with continuous stirring using magnetic stirrer. 5 mL of 1% trisodium citrate solution was preheated and quickly added to the boiling solution. A change in color was observed from yellowish to light purple and finally to dark purple after half an hour of boiling.

2.4 Concentration dependent synthesis of alloy nanoparticles

Synthesis of alloy nanoparticles with five different concentration ratios of gold and platinum salt was performed. Concentration ratios of gold and platinum salts were 100:0, 75:25, 50:50, 25:75 and 0:100 respectively, representing decrease in concentration of gold salt and increase in concentration of platinum salt. For these reactions, 0.7 mL of only gold salt in 8.8 mL distilled water was taken for 100:0 ratio of gold and platinum, 0.53 mL of gold salt and 0.18 mL of platinum salt in 8.8 mL distilled water for 75:25 ratio of gold and platinum, 0.35 mL of gold salt and 0.35 mL of platinum salt for 50:50 ratio of gold and platinum, 0.18 mL of gold salt and 0.53 mL of platinum for 25:75 ratio of gold and platinum, and finally 0.7 mL platinum salt only for 0:100 ratio of gold and platinum respectively. 1% (0.5 mL) trisodium citrate was used for all reactions.

2.5 Time dependent reduction of alloy nanoparticles

In this scheme, time of addition of trisodium citrate was varied from 1 second to 10 minutes. For 1 s, quick addition of 0.5 mL 1% trisodium citrate was added into reaction mixture. For 10s addition, 10 seconds were required for injection of trisodium citrate. Time was measured by a stopwatch. For 1 min, 5 min and 10 minutes same procedure was adopted.

2.6 Temperature dependent synthesis of alloy nanoparticles

Synthesis of alloy nanoparticles was also performed by varying the temperature conditions. These reactions were performed by maintaining temperatures at different levels of 50°C, 60°C, 70°C, 80°C, 90°C and 100°C, using 50:50 ratio of Au and Pt salts using quick addition of trisodium citrate to check the effect of temperature on size of alloy nanoparticles.

2.7 pH dependent synthesis of alloy nanoparticles

For pH dependent reactions, pH of both gold and platinum salt was adjusted by using 0.1M solution of sodium hydroxide. Initially, 0.35 mL of 0.01M solution gold salt and 0.35 mL of 0.01 M platinum salt was added to 8.8 mL of distilled water for the synthesis of alloy nanoparticles, pH was found to be around 3. Same amount of gold and platinum salt was kept for all pH dependent reactions. To adjust pH at 4, 7, 8 and 10, 67 µl, 170 µl, 180 µl and 190 µl of prepared 0.01 M sodium hydroxide was added to reaction mixture respectively to find out effect of pH on size of alloy nanoparticles.

2.8 Characterization of synthesized Au NPs, Pt NPs and alloy NPs

2.8.1 UV-Visible Spectroscopy

A T+80 PGI UV-Vis double beam spectrophotometer

was used for UV-Vis spectroscopy. The spectrophotometer wavelength range was from 190-1100 nm with +/- 0.3 nm wavelength accuracy containing deuterium and tungsten lamps. For sample, 10 mm path length of quartz cuvettes were used. The surface plasmon resonance (SPR) of Au NPs, Pt NPs and Au-Pt NPs were analyzed.

2.8.2 Scanning Electron Microscopy (SEM) & Energy-dispersive X-ray Spectroscopy (EDX)

A MIRA3 TESCAN-SEM with magnification range 20× to 30,000× with a resolution of 1 nm was used for characterization of size of nanoparticles.

2.8.3 X-Ray Diffraction (XRD)

A Bruker D8 Advance X-ray diffractometer with (Cu) Kα radiation wavelength (λ) of 1.5406 A° in the scan range (2θ) from 20°-70° with steps of 0.02° was used for the analysis of nanoparticles. The generator current was set at 30 mA with 40 kV voltage. The full width half maximum (FWHM) of peaks was obtained through X'Pert HighScore software. The matching of standard peaks was also performed through X'Pert HighScore software. The crystallite sizes were calculated using Scherrer's equation ($D = K\lambda/\beta cos\theta$) by using Microsoft Excel.

3. Results and discussion

3.1 Pure Au NPs synthesized by Turkevich method

Pure gold NPs (0.01 M, 0.7 mL) were synthesized by quick addition (1 s) of reducing agent giving SPR absorbance peak at 521 nm (Fig. 1). Quick addition of trisodium citrate reduces gold salt within a few seconds. Nucleation and growth was observed by change in color from yellowish to a beautiful wine-red color. The Haiss equation (Haiss *et al*. 2007) was used to calculate the size of Au NPs which were observed to be around 24 nm.

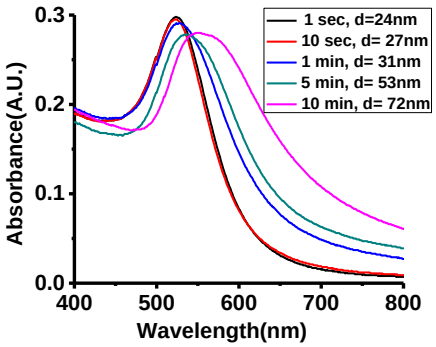

Fig. 1 UV-Vis spectra of Au NPs with different time of addition of citrate

3.2 UV-Vis spectrum of Au NPs with different time of addition of citrate

Fig. 1 shows the UV-Vis spectrum of pure gold NPs which were synthesized by the addition of reducing agent with different addition times. A bathochromic shift was observed for the absorption of SPR peaks at 521 nm, 525 nm, 528 nm, 534 nm and 553 nm for 1 s, 10 s, 1 min, 5 min and 10min of addition of citrate respectively. Absorption in this range shows the formation of gold nanoparticles. The size of the gold nanoparticles were calculated using Haiss equation $\left(d = \frac{ln\left(\frac{\lambda spr - \lambda_0}{L_1}\right)}{L_2}\right)$ where d is the diameter of the Au NPs, λ_{spr} is wavelength at the surface plasmon resonance peak, λ_o is fixed at 512, L_1 is fixed at 6.53 and L_2 is fixed at 0. 0216) (Haiss *et al*. 2007). The calculated size was 24 nm, 27 nm, 31 nm, 53 nm and 72 nm for 1 s, 10 s, 1 min, 5 min and 10 min respectively. For the citrate addition time of up to 1 min, the initial increase in size was small in the range of 3-4 nm for each delayed addition, due to nearly similar reduction rate. However, at longer time of addition of citrate, i.e., 5 and 10 minutes, the increase in size observed was approximately 20 nm for each delayed addition. This is because nucleation occurs in relatively small numbers initially (minute reducing agent is present in the beginning). Delayed addition of reducing agent causes growth to larger nanoparticles as sufficient time is available for the growth of each nanoparticle. In addition to that, formation of new small crystals also occurs which causes heterogeneity in size of nanoparticles obtained.

3.3 XRD analysis of Au NPs synthesized by varying time of addition of citrate

Fig. 2 below shows XRD patterns of pure Au NPs synthesized with different time of addition of trisodium citrate. 1s and 1min addition of trisodium citrate (Fig. 2) shows characteristic peaks of Au NPs at 2θ value of 38.18° which matches with the standard pattern for Au NPs (JCPSD 04-0784). The size for AuNPs was calculated using Scherrer's equation (Essinger-Hileman *et al*. 2011). The calculated size for 1 s and 1 min was 21 nm and 29 nm respectively and shows face centered cubic (fcc) crystal structure. XRD peaks at 2θ value of 38.18°, 44.38°, and 64.57° represented by their Miller indices (111), (200), and (220) assigned to Au NPs (JCPSD 65-2870). Peak at 2θ value of ~46° is due to the glass substrate. Most intense peak (111) with different time of addition of citrate was observed at 38.18°. These results show that increase in time of addition of reducing agent results in increase in crystallite size of AuNPs as was observed from UV-Vis spectroscopy. One example (Au NPs; 1 sec addition of reducing agent) for calculating the crystallite size is shown

Table 3 Comparison of Au-Pt NPs (50:50) sizes and elemental composition obtained through different characterization techniques

β (FWHM)	Rad β (FWHM)	2θ	θ	Rad θ	cosθ	β cosθ	Crystallite size (nm)
0.3936	0.0068724	38.1438	19.0719	0.333	1	0.0068722	~21

Fig. 2 XRD spectrum of Au NPs with different time of addition of reducing agent

below. The rest of the samples were calculated similarly for their crystallite sizes.

$D = K\lambda/\beta\cos\theta$ (Scherrer Equation), where $K = 0.9$; $\lambda = 1.5406$

3.4 SEM images of pure Au NPs with different time intervals of citrate addition

Fig. 3 below shows the SEM images of Au NPs synthesized at 1 second and 10 min addition time of citrate, representing an increase in average particle size from 25 nm to 67 nm respectively. The scales are also provided with each image. The sizes observed are similar to as observed from UV-Vis spectroscopy and XRD.

The increase in time of addition of citrate allows particles size to increase due to growth of nanoparticles as citrate reduces salt on already present nanoparticles.

3.5 EDX results of Au NPs with time of addition of citrate

Fig. 4 below shows EDX results of pure Au NPs showing the elemental composition of gold in Au NPs synthesized with different time of addition of citrate.

EDX results shows the presence of Au which confirms the reduction of gold salt with time of addition of citrate for 1 s and 10 min. Si peak was also found in EDX spectrum which was due to the presence of glass.

The comparison of size through different characterization techniques for Au NPs has been summarized in Table 1 below.

3.6 Synthesis of platinum nanoparticles

Fig. 5 represents the UV- Vis spectrum of platinum

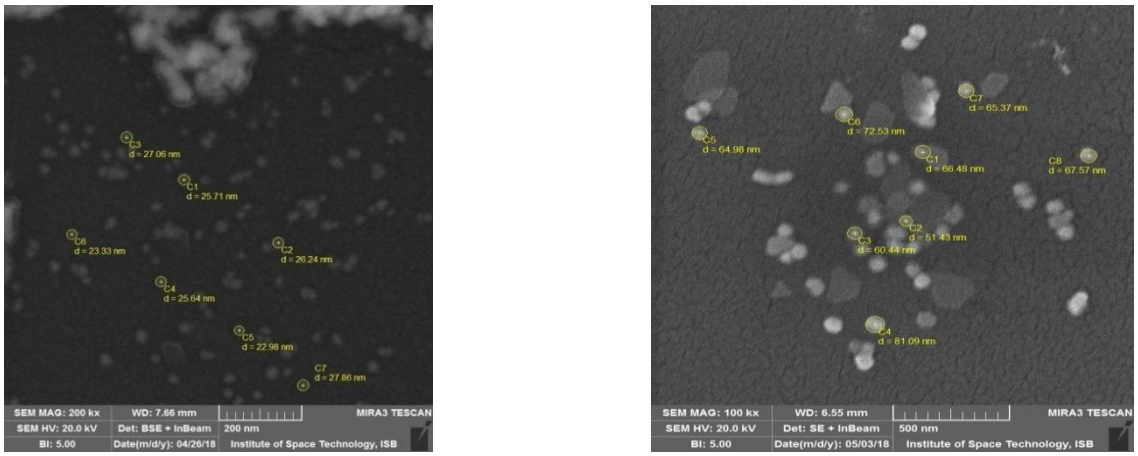

Fig. 3 SEM images of Au NPs with different time intervals for 1 s (left) and 10 min (right)

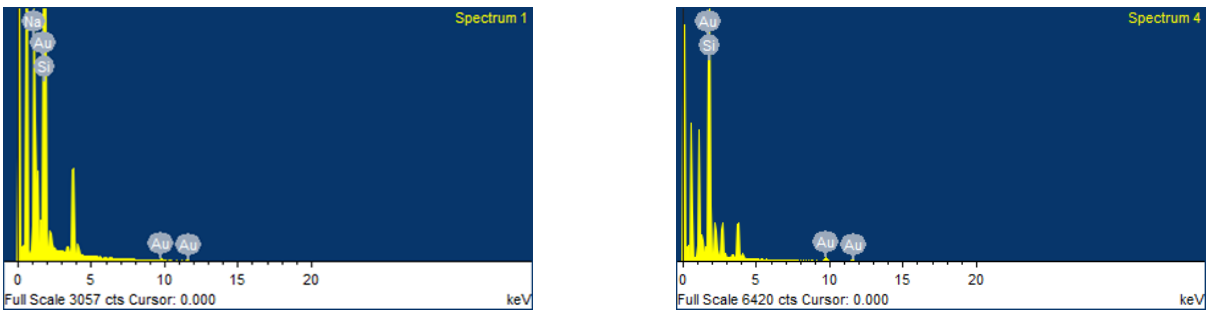

Fig. 4 Elemental composition of Au NPs with different time of addition of citrate for 1 s (left) and 10 min (right)

Table 1 Comparison of AuNPs sizes obtained through various techniques

Time	UV-VIS	XRD	SEM	EDX
1 sec	24 nm	21 nm	25 nm	100%
10 sec	27 nm	-	-	-
1 min	31 nm	29 nm	-	-
5 min	53 nm	-	-	-
10 min	72 nm	-	67 nm	100%

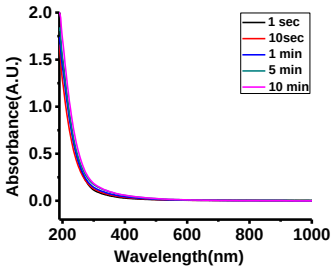

Fig. 5 UV-Vis spectra of pure Pt NPs at different time of addition of citrate

nanoparticles which were synthesized by reduction of platinum salt (100%, 0.01 M, 0.7 mL) using trisodium citrate. The synthesized Pt NPs were confirmed by change in color from yellowish color to a colorless solution and then finally brown colored solution, representing formation of Pt nanoparticles. Pt nanoparticles have no characteristic SPR peak which is also known in literature (Ali and Ahmed 2018). Moreover, the reduction rate of platinum salt is very slow as compared to gold and requires longer time for formation of nanoparticles.

3.7 UV-Vis spectra of Pt NPs by varying time of addition of citrate

Fig. 5 represents UV-Vis spectrum of pure Pt NPs which were synthesized by reduction of platinum salt (0.01 M, 100%, 0.7 mL) using trisodium citrate (1%, 0.5 mL) with different time of addition of citrate in 1 s, 10 s, 1 min, 5 min and 10 min respectively. Change in time of addition of citrate from 1s to 10 min, the absorbance peaks show no significant difference. Pt NPs synthesized at 1 s, 10 s, 1 min, 5 min and 10 min shows maximum absorbance of 1.662, 1.744, 1.751, 1.839 and 2.002 respectively.

3.8 XRD analysis of Pt NPs synthesized by varying time of addition of citrate

Fig. 6, given below, shows XRD patterns of pure Pt NPs which were synthesized by reduction of platinum salt (0.01 M, 0.7 mL in 8.8 mL DDW) with varying time addition of citrate (1%, 5 mL). For all Pt NPs synthesized at 1 s, 10 s, 1 min, 5 min and 10 min, one diffraction peak (200) at 2θ value of 46.23 was observed which matches with standard pattern (JCPDS 65-2868). The most intense peak (200) was used to calculate the crystallite size in all the given spectra using Scherer's equation. For 1 s, 10 s, 1 min, 5 min and 10 min, the calculated size was 15 nm, 18 nm, 30 nm, 54 nm and 95 nm respectively having face centered cubic (fcc) crystal structure. Set of diffractions at 2θ value of 39.75°,46.23°, 57.0° and 67.45° (JCPDS65-2868) were characterized by their Miller indices (111), (200), (110) and (112) respectively. These results show that with increase in time of addition of citrate, increase in particle size is observed due to the agglomeration of particles or growth of already formed nanoparticles along with new particles formation at the same time and causes non-uniformity with larger particle sizes as observed in the later examples.

The comparison of sizes of Pt NPs synthesized at different time of addition of reducing agent are summarized in Table 2 below.

3.9 Synthesis of Au-Pt alloy nanoparticles

Alloy nanoparticles of gold and platinum were synthesized by using standard method (Essinger- Hileman

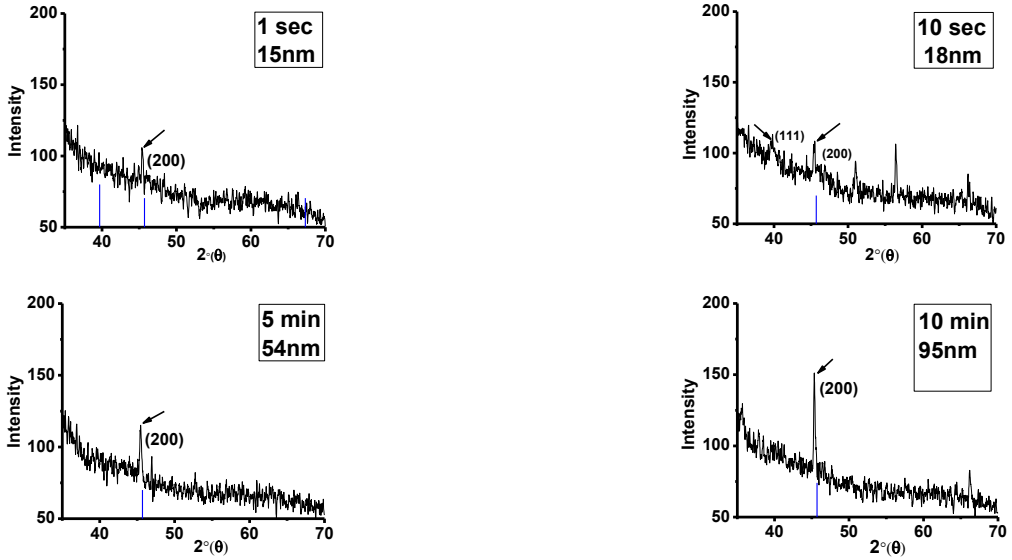

Fig. 6 XRD patterns of pure Pt NPs

Table 2 Crystallite size calculation of Pt NPs obtained by change in time of addition of reducing agent

Time	Size
1 sec	15 nm
10 sec	18 nm
1 min	30 nm
5 min	54 nm
10 min	95 nm

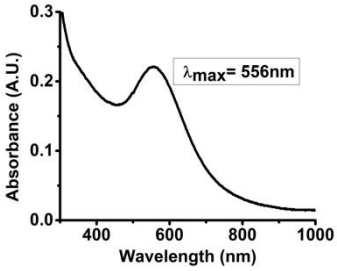

Fig. 7 Vis spectrum of Au-Pt alloys NPs with fast addition of trisodium

et al. 2011), in which trisodium citrate was used as reducing agent as well as capping agent. Fig. 7 represents UV-Vis spectrum of alloy nanoparticles with equal concentration of gold and platinum with SPR peak at 556 nm.

3.10 Alloy nanoparticles with 50% gold and 50% platinum

UV-Vis spectrum of $Au_{50}Pt_{50}$ alloy nanoparticles, synthesized by taking 50% of gold salt (0.01 M, 0.35 mL) and 50% of platinum salt (0.01 M, 0.35 mL) is shown in Fig. 8 below. Reducing agent (1%, 0.5 mL) was added in varying timings of 1 s, 10 s, 1 min, 5 min and 10 min into to boiling salt solution respectively.

Fig. 8 shows SPR of alloy nanoparticles which was shifted from 541 nm to 578 nm for 1 s to 10 min respectively. This confirms the formation of alloy nanoparticles, where size is proportional to time of addition of trisodium citrate. For 1 s, size of nanoparticles was small because of quick reduction and stabilization of citrate. However, for 10 min addition of citrate, particles size was found to be large as observed from the bathochromic shift of the peaks. This increase in size with increase in time of addition of reducing agent was possibly due to simultaneous growth of nanoparticles due to further addition of citrate. In the beginning, salt was reduced by small amount of trisodium citrate and complete stabilization of citrate was not possible. Further slow addition of citrate results in growth of seeds to large NPs and also formation of new nanoparticles resulting in heterogeneity in size of alloy nanoparticles. Generally, we can conclude that bathochromic shift was observed representing increase in size and increase in homogeneity with delayed time of addition of citrate.

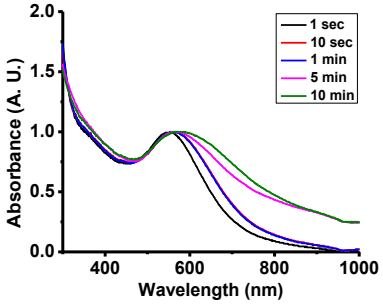

Fig. 8 UV-Vis spectra of $Au_{50}Pt_{50}$ with different time of addition of citrate

3.11 XRD analysis of alloy nanoparticles with 50% gold and 50% platinum

XRD spectra of alloy nanoparticles at 1s and 5min with addition of trisodium citrate is shown in Fig. 9 below. Two characteristic peaks were observed for 1s at 2θ value of 38.18° (111) and 65.65° (220) respectively and for 5 minutes three characteristic peaks were found at 2θ values of 38.18° (111), 44.35° (200) and 64.55° (220) respectively. Most intense peak was used for size calculations by Scherer's equation ($D = K\lambda/\beta cos\theta$, where, D is the mean crystallite size, K is a dimensionless shape factor, with a value of 0.9, λ is the X-ray wavelength, β is the line broadening at half the maximum intensity (FWHM) (also denoted as 2θ) and θ is the Bragg's angle, all calculated in radians. A sample calculation is shown in section 3.3). The calculated crystallite size was 38 nm for 1 s and 45 nm for 5 min addition of citrate.

Alloy nanoparticles matching with the standard patterns with set of diffractions for Au-Pt alloy nanoparticles at $\boldsymbol{2\theta}$ value of 38.18°, 44.35°, and 64.65° were characterized by their (111), (200), and (220) Miller indices respectively (Xu *et al*. 2008) are shown in Fig. 9 above. Change in time

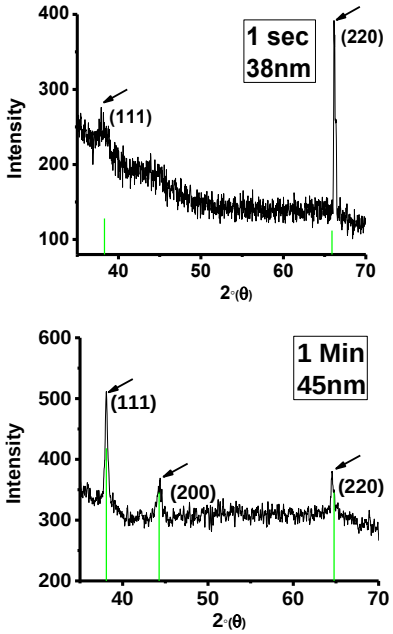

Fig. 9 XRD spectrum of $Au_{50}Pt_{50}$ with different time of addition of citrate

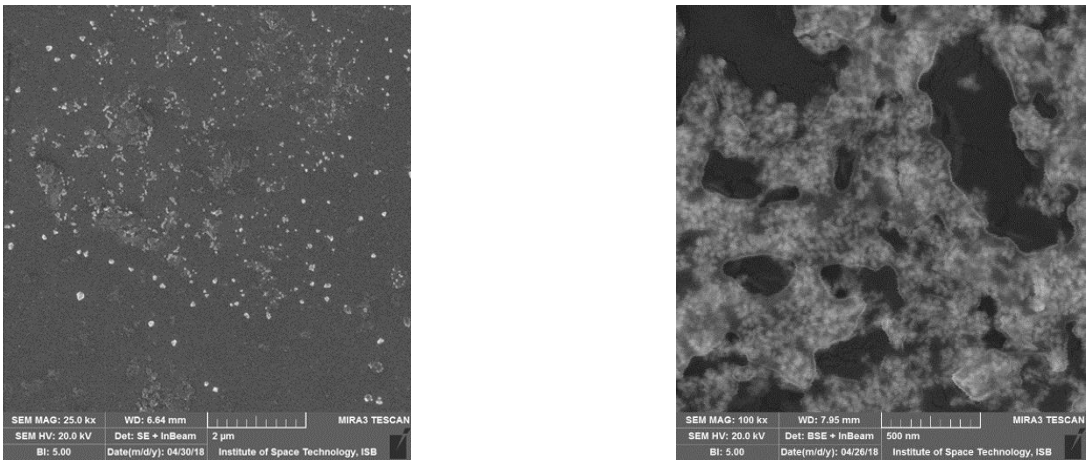

Fig. 10 SEM images of Au-Pt NPs with (a) 1 sec and (b) 5 min of citrate addition

of addition of trisodium citrate from 1 s to 10 min also changes the size of Au-Pt NPs as for 1 s, reducing agent quickly reduced and stabilized NPs. For 5 min addition time of citrate, reduction occurs slowly, which allows increase in size of alloy nanoparticles due to continuous growth of nanoparticles.

3.12 SEM images of 50% gold and 50% platinum alloy nanoparticles with different time of addition of citrate

SEM images of Au-Pt alloys nanoparticles (50: 50) at 1s and 5 min time of addition of citrate, representing an average particle size of 30 nm and 37 nm respectively. Respective scales are also provided with SEM images.

SEM results for gold and platinum alloy nanoparticles (50:50) with varying time of addition of citrate for 1 s and 5 min are shown in Fig. 10 above. Size of alloy nanoparticles was found to be 30 nm for 1s citrate addition and 37 nm for 5 min citrate addition respectively. The increase in size was due to growth of nanoparticles with slow addition of citrate.

3.13 EDX results of 50% gold and 50% platinum alloy nanoparticles with different time of addition of citrate

Elemental composition (EDX spectra) of Au-Pt (50: 50) alloy nanoparticle at 1 second, 1 minute and 5 minute with addition of time of trisodium citrate (Fig. 11), shows Au-Pt (50:50) 99.97% gold and 0.03% platinum for 1 s, for 1 min Au was 89.83% and Pt was 10.17% and for 5 min Au was 79.7% and 20.29% platinum respectively.

EDX results for gold and platinum alloy nanoparticles (50:50) shows that percentage of gold decreases while percentage of platinum increases for increase in time of addition of reducing agent. The size of alloy NPs also increases with increase in platinum concentration. For 1s there was quick addition of citrate which increases gold percentage in alloy nanoparticles, probably formation of core-shell structures with platinum inside and gold outside. For 1 min, a small change was observed. However, for 5min addition of citrate, percentage of gold was decreased to about 79.7% and platinum percentage was increased to 20.29%. This is due to lower amount of citrate forms gold nanoparticles initially and further slow addition of citrate brings platinum on the surface of nanoparticles.

The comparison of sizes and elemental ratio of Au-Pt NPs synthesized in 50:50 ratio, obtained through various techniques have been summarized in Table 3 below.

Table 3 Comparison of Au-Pt NPs (50:50) sizes and elemental composition obtained through different characterization techniques

Time	XRD	SEM	EDX
1 sec	38 nm	30 nm	99.97%Au, 0.03% Pt
5 min	45 nm	37 nm	79.7% Au, 20.3% Pt

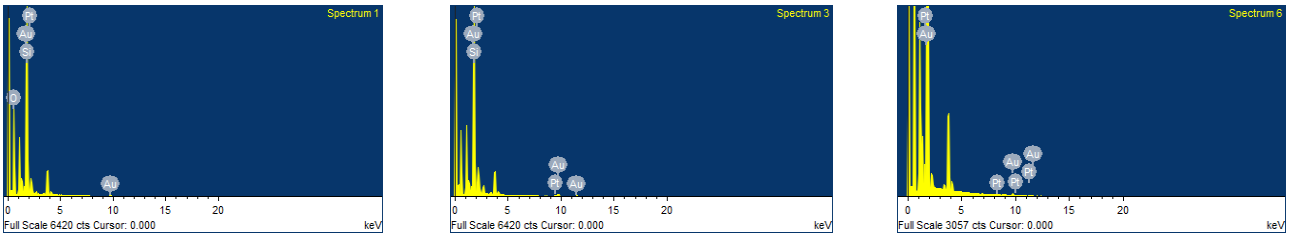

Fig. 11 Elemental composition of Au and Pt in $Au_{50}Pt_{50}$

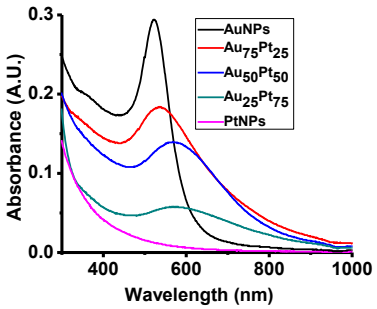

Fig. 12 UV-Vis spectrum of ratio dependent synthesis of Au-Pt alloys NPs

(Au:Pt), 25:75 (Au:Pt) and 0:100 (Au:Pt) with reducing agent are shown in Fig. 12 above.

A bathochromic shift was observed for SPR peaks in the range of 523 nm to 579 nm with increasing range of 523 nm to 579 nm with increasing concentration of platinum in the alloy nanoparticles. This also indicates the formation of alloy nanoparticles. For 100 percent gold salt, SPR peak was observed at 523 nm which shows formation of gold nanoparticles. For gold and platinum alloy nanoparticles in the ratio of 75:25 (Au:Pt), SPR was observed at 535 nm; SPR peak of 50:50 (Au:Pt) was observed at 556 nm, and SPR peak of 25:75 (Au:Pt) was observed at 567 nm which shows possible increase in size of alloy NPs. It is also important to mention that the intensity of SPR peak decrease with increasing concentration of platinum nanoparticles because this SPR is representative of Au present in the alloy nanoparticles. For 0:100 (Au-Pt) no SPR peak was found because platinum nanoparticles have no such characteristic SPR peak. The size of gold and platinum alloy nanoparticles increases with increasing concentration of Pt NPs due to the presence of miscibility gap between the two elements.

3.15 XRD analysis of ratio dependent synthesis of Au-Pt alloy nanoparticles

XRD patterns of pure gold, alloy and platinum nanoparticles synthesized at different ratios (100:0, 75:25, 50:50, 25:75 and 0:100) are shown in Fig. 13 below. Pure gold nanoparticles show characteristic peaks at 2θ value of 38.18° (111); matching with the standard pattern for Au NPs (JCPSD 04-0784). Gold and platinum alloy nanoparticles (75:25) show one characteristic peak at 2θ value of 45.00° (200) Miller indices plane. For 50:50 (Au-Pt) gives two characteristic peaks at 2θ value of 38.8° and 65.65° representing by (111) and (220) planes. Au-Pt alloy nanoparticles (25:75) gives one characteristic peak at 2θ value of 65.65° marked by (220). Finally, pure platinum nanoparticles give one characteristic peak at 2θ value of 46.23° representing (200) plane. The most intense peak was selected for size calculations of nanoparticles by Scherer's equation. The calculated size obtained for Au-Pt (100:0, 75:25, 50:50, 25:75 and 0:100) was 21 nm, 30 nm, 38 nm, 89 nm and 15 nm respectively. The most interesting aspect is the change in the planar structure of these nanoparticles on changing the ratio of Au and Pt. This essentially means that changing ratio results in the different crystallite structures along with increase in size of nanoparticles.

It has been observed that monometallic nanoparticles have smaller sizes as compared to the alloy nanoparticles and size of Au-Pt alloy nanoparticles increase with increasing platinum content. This increase in size of Au-Pt NPs is due to the presence of miscibility gap between the gold and platinum. This miscibility gap exists because of different reduction kinetics (Shim *et al*. 2019) and interatomic distances between the two different size of atoms. (Chatzidakis *et al*. 2017)

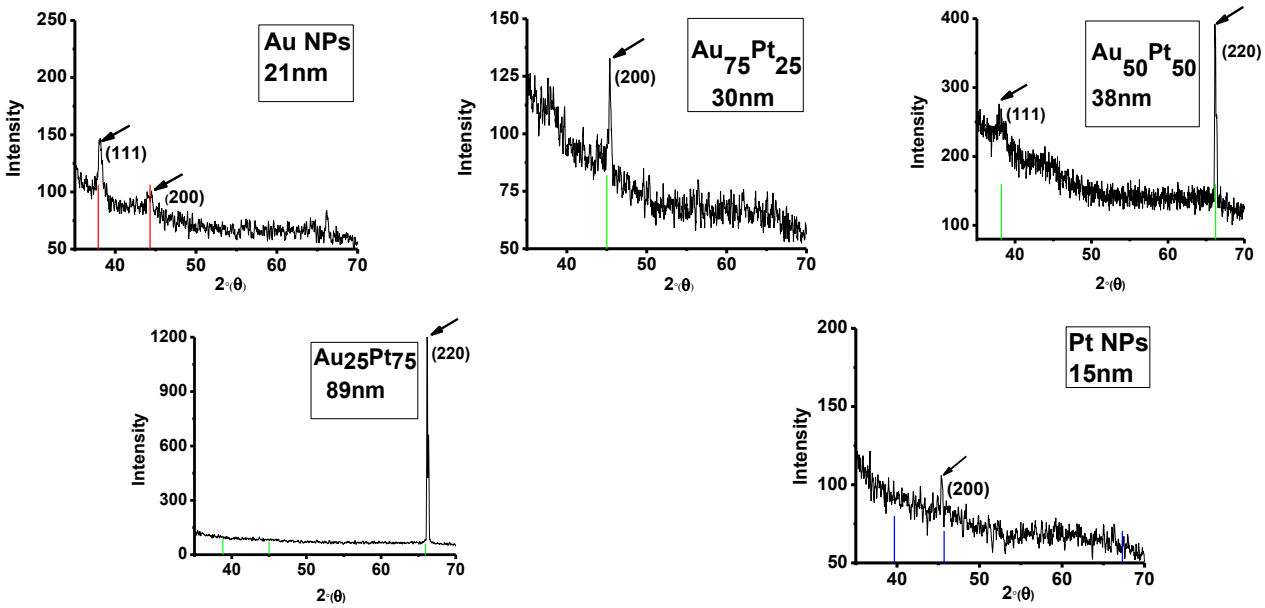

Fig. 13 XRD spectrum of concentration dependent synthesis of Au-Pt alloy nanoparticles

Table 4 Comparison of NP sizes obtained through various techniques

Ratio	XRD	SEM	EDX
AuNPs	21 nm	25 nm	-
$Au_{75}Pt_{25}$	30 nm	30 nm	Au 91.55%, Pt 8.45%
$Au_{50}Pt_{50}$	38 nm	30 nm	Au 77.32%, Pt 22.68%
$Au_{25}Pt_{75}$	89 nm	90 nm	Au 69.09%, Pt 30.91%
PtNPs	15 nm	-	-

3.16 EDX analysis of Au NPs and Au-Pt NPs with different ratios of salts

Elemental composition by EDX analysis of gold and platinum in the Au-Pt NPs, synthesized with different ratios of gold and platinum salt (75:25, 50:50, and 25:75) shows direct proportionality to the concentration of both salts in the precursor salt solution, as provided in Table 4 above. However, the percentage of gold is much higher as compared to the platinum content, because the reduction rate of gold is higher than that of platinum in addition to the miscibility gap discussed previously. EDX analysis also confirms the structure of Au-Pt NPs i.e., with increasing Pt percentage, the content of platinum increases on the shell, however gold has preference to be in core due to greater reducing abilities of gold salt as compared to platinum salt.

The size and elemental ratio of Au-Pt NPs obtained through various techniques is summarized in Table 4 above.

3.17 Alloy nanoparticles with 75% gold and 25% platinum

UV-Vis spectrum of alloy nanoparticles synthesized by using 75% gold (0.01 M, 0.525 mL) and 25% platinum (0.01 M, 0.175 mL) at 100°C with reducing agent (trisodium citrate) added at varying times of 1 s, 10 s, 1 min, 5 min and 10 min is shown below in Fig. 14. The SPR peak observed was shifted from 529 nm to 572 nm.

SPR peaks were observed at 529 nm, 540 nm, 554 nm, 560 nm and 572 nm respectively. Bathochromic shift along with peak broadening was observed from 1 s to 10 min which shows that the size of the particles is in increasing order. Formation of alloy nanoparticles shows gold in higher amount as expected and SPR peak for short addition timings shows formation of small size of alloy nanoparticles, where reducing agent was able to reduce salts and stabilize nanoparticles quickly. Slow addition of citrate causes large size of alloy nanoparticles because of miscibility gap as well as growth of already formed nanoparticles on addition of citrate at later times. Additionally, increase in heterogeneity of nanoparticles is also evident due to broadening of peaks which is due to formation of new nanoparticles along with growth of previously formed nanoparticles at higher addition time of citrate.

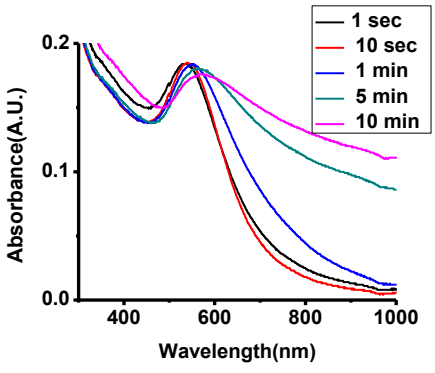

Fig. 14 UV-Vis spectra of $Au_{75}Pt_{25}$ *synthesized* at specific time intervals

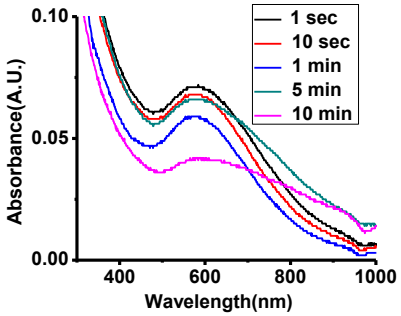

Fig. 15 UV-Vis spectrum of $Au_{25}Pt_{75}$ alloy nanoparticles

3.18 Alloys nanoparticles with 25% gold and 75% platinum

UV-Vis spectrum of gold (0.01 M, 0.175 mL) and platinum (0.01 M, 0.525 mL) alloy nanoparticles synthesized at 100°C with trisodium citrate (1%, 0.5 mL), which was added at varying times of 1 s, 10 s, 1 min, 5 min and 10 min respectively, is shown in Fig. 15 above.

A relatively minor bathochromic shift of SPR peaks along with hypochromic shift was observed from 548 nm to 563 nm (1 s - 10 min) which shows formation of alloy nanoparticles having higher percentage of platinum. SPR peak of alloy nanoparticles was found at 548 nm, 554 nm, 558 nm, 560 nm and 563 nm for 1 s, 10 s, 1 min, 5 min and 10 min respectively representing increase in size. Broadening of SPR peak was observed for 5 min and 10 min addition of citrate as expected due to heterogeneity of nanoparticles formed. As soon as the size is increased, relatively lower concentration of nanoparticles is formed,

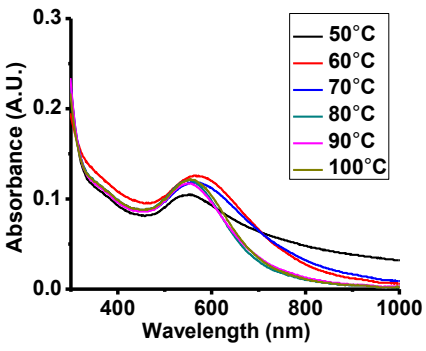

Fig. 16 UV-Vis spectrum of temperature dependent alloy nanoparticles

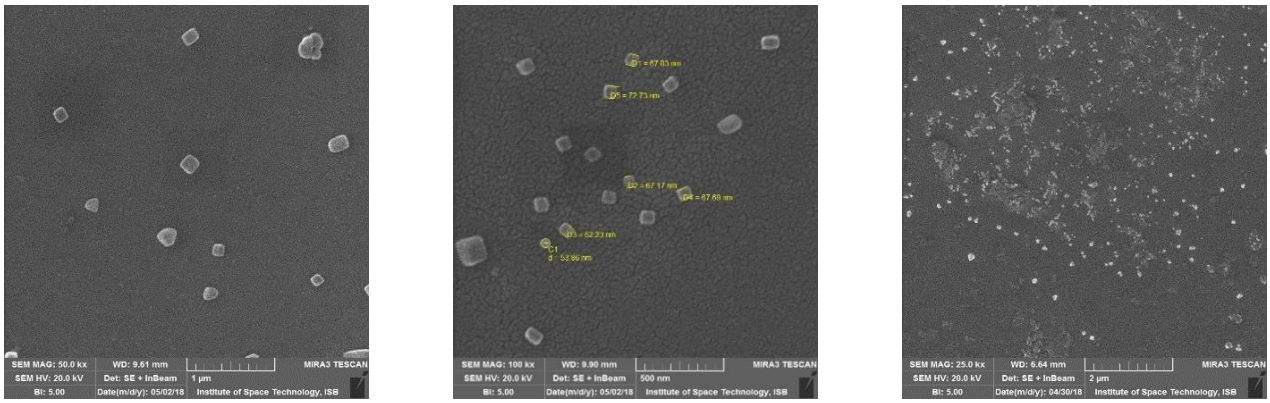

Fig. 17 SEM images of Au-Pt alloy nanoparticles at 60°C, 80°C and 100°C

Table 5 Percentage composition of gold and platinum in Au-Pt NPs synthesized at different temperatures

Temp	Au (%)	Pt (%)
60°C	100	0
70°C	91.55	8.45
80°C	77.32	22.68
90°C	81.24	18.76
100°C	92.24	7.7

which also causes hypochromic shift in the SPR peaks. This could also be due to agglomeration occurring for unstable nanoparticles.

3.19 Temperature dependent synthesis of alloy nanoparticles

Fig. 16 above shows UV-Vis spectrum of alloy nanoparticles with equal ratio of gold and platinum salts at different temperatures ranging from 50°c to 100°C. A hypsochromic shift is observed from 572 nm to 548 nm for nanoparticles synthesized from 60°C to 100°C, which represents a better control in morphology at higher temperatures. At 50°C, the peak was observed at 548 nm. Peaks at 80°C and above are narrower representing homogeneity in the size of nanoparticles, which is due to efficient reduction and capping of trisodium citrate at higher temperatures. Broad peaks are observed at 50°C-70°C, representing increase in heterogeneity of size at lower temperatures. The broadening and decrease in intensity of SPR peak at 50°C is due to agglomeration where incomplete reduction of salts occurs and less control in size of nanoparticles is observed.

The comparison of elemental ratio of Au-Pt NPs, obtained at various temperatures is summarized in Table 5 above.

3.20 SEM images of temperature dependent alloy nanoparticles

SEM images of gold and platinum alloy nanoparticles at 60°C, 80°C and 100°C showing an average particle size of 120 nm, 70 nm and 30 nm respectively are shown above

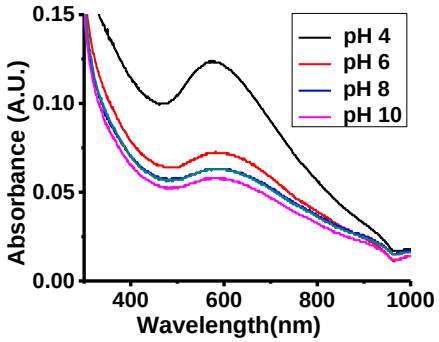

Fig. 18 UV-Vis spectrum of pH dependent gold and platinum alloy nanoparticles

(Fig. 17). Scales are provided with images.

SEM images of Au-Pt alloy nanoparticles synthesized at 60°C show size of 120 nm. At low temperature, capping and reduction of gold and platinum salt with trisodium citrate is not efficient, which causes increase in size of nanoparticles. However, increase in temperature causes efficient reduction and capping, which results in decrease of particle size. At temperature 80°C and 100°C, size of Au-Pt alloy nanoparticles observed were 70 nm and 30 nm respectively.

3.21 pH dependent synthesis of alloy nanoparticles

SPR of gold and platinum alloy nanoparticles synthesized at different pH values of 2, 4, 6, 7, 8 and 10 was observed. A minute bathochromic shift of SPR peaks along with broadening was observed from 576 nm to 589 nm for pH 4 to pH 10 respectively as shown in Fig. 18, however the intensity of the peaks was continuously decreased.

Agglomeration was observed for reaction at pH 2 due to addition of HCl. At pH 4 uniformly distributed small sized Au-Pt NPs were observed as evident by narrow peaks. At pH values of 6, 8 and 10, relatively larger particles were formed along with heterogeneity in size of nanoparticles as evidenced by increase in broadness and decrease in intensity of SPR peaks. The larger particle size with increase in pH is due to the increase in the basic character of reducing agent causing increase in the reduction rate of

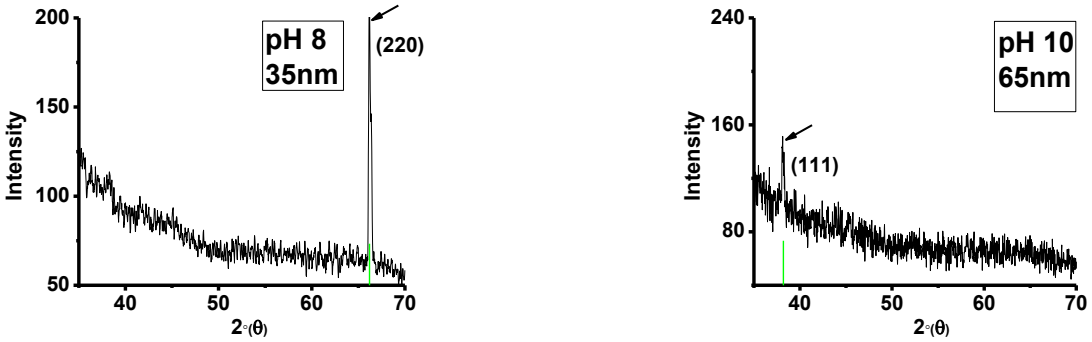

Fig. 19 XRD spectrum of pH dependent synthesis of Au-Pt alloy nanoparticles

Pt that appears on the surface, which also causes decrease in the intensity of SPR peaks.

3.22 XRD analysis of pH dependent synthesis of Au-Pt alloy nanoparticles

XRD patterns of two representative samples of gold and platinum alloy nanoparticles synthesized with ratio of 1:1 at pH values of 8 and 10 with quick addition of reducing agent are shown in Fig. 19 above.

Alloy NPs formed at pH 8 and pH 10 gives characteristic peaks at 2θ values of 38.8° and 65.65° with (111) and (220) planes respectively, representing face centered cubic (fcc) crystal structure. The crystallite size was calculated by using Scherer's equation. Size of alloy nanoparticles at pH 8 was 35 nm and at pH 10 was 65 nm. Increase in particle size with increase in pH was due to increase in the basic character of trisodium citrate, which becomes strong reducing agent and causes agglomeration resulting in larger particle sizes.

4. Conclusions

Gold, platinum and Au-Pt alloy nanoparticles were synthesized by Turkevich method using trisodium citrate as reducing and capping agent. Gold nanoparticles of size 23±2 nm were observed with SPR peak at 524 nm, whereas platinum nanoparticles of 15 nm were observed without any characteristic SPR peak. Various characterization techniques including UV-Vis spectroscopy, XRD, SEM, and EDX were used to characterize nanoparticles including their size and elemental composition. For the effects on size of Au NPs, Pt NPS and Au-Pt NPs, the effect of various factors such as time of addition of reducing agent, ratios of salts, temperature conditions for NP synthesis, and pH conditions for NP synthesis were studied. In general, the Turkevich method involves fast addition of 1% trisodium citrate to the boiling precursor salt solution, which results in the synthesis of small and homogenous sized nanoparticles. In the present study, it was very interesting to study change in addition time (fast to very slow addition) of citrate to the boiling salt solution. The addition of citrate timings were changed gradually from 1 second to 10 minutes or in other words, from very slow addition to very fast addition. This affected the size of nanoparticles, where all types of nanoparticles synthesized at different ratios of gold and platinum (Au:Pt :: 100:0, 75:25, 50:50, 25:75, 0:100) show increase in size with increasing addition time of citrate. This is mainly due to growth of already formed nanoparticles on further addition of citrate at later times. Simultaneously, new particles form which results in non-homogeneous formation of nanoparticles, mainly at 5 min and 10 min addition of citrate. Another interesting factor was observed through EDX spectroscopy, where gold was always in higher ratio as compared to platinum at the shell of the nanoparticles, however, platinum content increases with increasing time of addition of citrate. This is attributed to miscibility gap of Au and Pt, where Pt has tendency to remain in core and Au on shell, however at higher citrate addition timings, platinum content is increased on shell due to slow reduction process.

Au-Pt alloy nanoparticles' SPR peaks continuously decrease as the content of Pt is increased because Pt does not have any characteristic SPR peak. The size of Au-Pt bimetallic alloy nanoparticles is also directly affected by the ratio of metal salts in the precursor solution. It has been observed that monometallic nanoparticles have smaller sizes as compared to the bimetallic alloy nanoparticles and the size of Au-Pt bimetallic alloy nanoparticles increase with increasing platinum content. Furthermore, Au-Pt (50:50) NPs were also synthesized at different temperatures of 50°C, 60°C, 70°C, 80°C, 90°C and 100°C. UV-Vis spectrum of Au-Pt (50:50) alloy nanoparticles synthesized at these temperatures show a blue shift representing decrease in size of nanoparticles as temperature is increased, which was also confirmed by SEM studies. The additional effect observed for the temperature studies was homogenous size formation of nanoparticles at higher temperatures and heterogenous size nanoparticles formation at lower temperatures. Finally, Au-Pt NPs synthesized at pH values ranging from 4 to 10 shows an increase in size with increasing pH. This increase in size is due to the increase in basic character of reducing agent at higher pH values.

Acknowledgments

The research described in this paper was financially supported by the Higher Education Commission of Pakistan under National Research Program for Universities with reference no. 20-3369/R&D/HEC/14/978.

References

Ali, A. and Ahmed, S. (2018), "Green Synthesis of Metal, Metal Oxide Nanoparticles, and Their Various Applications", In: *Handbook of Ecomaterials*, Springer, pp. 1-45.

Anicetus Muche, T. (2010), *Synthesis, characterisation and applications of bimetallic nanoparticles*, Unpublished, University of Birmingham.

Calvo, F. (2013), *Nanoalloys*: *From Fundamentals to Emergent Applications*, Newnes.

Chatzidakis, M., Prabhudev, S., Saidi, P., Chiang, C.N., Hoyt, J.J. and Botton, G.A. (2017), "Bulk Immiscibility at the Edge of the Nanoscale", *ACS Nano*, **11**(11), 10984-10991.

Chen, M., Liu, J.P. and Sun, S. (2004), "One-Step Synthesis of FePt Nanoparticles with Tunable Size", *J. Am. Chem. Soc.*, **126**(27), 8394-8395.

Choi, K.W., Kim, D.Y., Ye1a, S.J. and Park, O.O. (2014), "Shape- and size-controlled synthesis of noble metal nanoparticles", *Adv. Mater. Res., Int. J.*, **3**(4), 199-216.

Essinger-Hileman, E.R., DeCicco, D., Bondi, J.F. and Schaak, R.E. (2011), "Aqueous room-temperature synthesis of Au–Rh, Au–Pt, Pt–Rh, and Pd–Rh alloy nanoparticles: fully tunable compositions within the miscibility gaps", *J. Mater. Chem.*, **21**(31), 11599-11604.

Ferrando, R., Jellinek, J. and Johnston, R.L. (2008), "Nanoalloys: from theory to applications of alloy clusters and nanoparticles", *Chem. Rev.*, **108**(3), 845-910.

Haiss, W., Thanh, N.T.K., Aveyard, J. and Fernig, D.G. (2007), "Determination of Size and Concentration of Gold Nanoparticles from UV−Vis Spectra", *Anal. Chem.*, **79**(11), 4215-4221.

He, W., Han, X., Jia, H., Cai, J., Zhou, Y. and Zheng, Z. (2017), "AuPt Alloy Nanostructures with Tunable Composition and Enzyme-like Activities for Colorimetric Detection of Bisulfide", *Scientific Reports*, **7**, p. 40103.

Henglein, A., Ershov, B. and Malow, M. (1995), "Absorption spectrum and some chemical reactions of colloidal platinum in aqueous solution", *J. Phys. Chem.*, **99**(38), 14129-14136.

Huang, X., Jain, P.K., El-Sayed, I.H. and El-Sayed, M.A. (2007), "Gold nanoparticles: interesting optical properties and recent applications in cancer diagnostics and therapy".

Hwang, B.J., Senthil Kumar, S.M., Chen, C.-H., Chang, R.-W., Liu, D.-G. and Lee, J.-F. (2008), "Size and alloying extent dependent physiochemical properties of Pt− Ag/C nanoparticles synthesized by the ethylene glycol method", *J. Phys. Chem. C*, **112**(7), 2370-2377.

Kimling, J., Maier, M., Okenve, B., Kotaidis, V., Ballot, H. and Plech, A. (2006), "Turkevich method for gold nanoparticle synthesis revisited", *J. Phys. Chem. B*, **110**(32), 15700-15707.

Mathis, J.E., Kidder, M.K., Li, Y., Zhang, J. and Paranthaman, M.P. (2016), "Controlled synthesis of mesoporous codoped titania nanoparticles and their photocatalytic activity", *Adv. Nano Res., Int. J.*, **4**(3), 157-165.

Schabes-Retchkiman, P., Canizal, G., Herrera-Becerra, R., Zorrilla, C., Liu, H. and Ascencio, J. (2006), "Biosynthesis and characterization of Ti/Ni bimetallic nanoparticles", *Optical Mater.*, **29**(1), 95-99.

Shaikh, A.J., Batool, M., Yameen, M.A. and Waseem, A. (2018), "Plasmonic Effects, Size and Biological Activity Relationship of Au-Ag Alloy Nanoparticles", *J. Nano Res.*, **54**, 98-111.

Shim, K., Lee, W.-C., Heo, Y.-U., Shahabuddin, M., Park, M.-S., Hossain, M.S.A. and Kim, J.H. (2019), "Rationally designed bimetallic Au@Pt nanoparticles for glucose oxidation", *Scientific Reports*, **9**(1), p. 894.

Sun, L., Wang, H., Eid, K. and Wang, L. (2016), "Shape-controlled synthesis of porous AuPt nanoparticles and their superior electrocatalytic activity for oxygen reduction reaction", *Sci. Technol. Adv. Mater.*, **17**(1), 58-62.

Valodkar, M., Modi, S., Pal, A. and Thakore, S. (2011), "Synthesis and anti-bacterial activity of Cu, Ag and Cu–Ag alloy nanoparticles: a green approach", *Mater. Res. Bull.*, **46**(3), 384-389.

Wang, W., Zheng, D., Du, C., Zou, Z., Zhang, X., Xia, B., Yang, H. and Akins, D.L. (2007), "Carbon-supported Pd-Co bimetallic nanoparticles as electrocatalysts for the oxygen reduction reaction", *J. Power Sources*, **167**(2), 243-249.

Wu, M.-L., Chen, D.-H. and Huang, T.-C. (2001), "Preparation of Au/Pt Bimetallic Nanoparticles in Water-in-Oil Micro-emulsions", *Chem. Mater.*, **13**(2), 599-606.

Xu, J., Zhao, T., Liang, Z. and Zhu, L. (2008), "Facile preparation of AuPt alloy nanoparticles from organometallic complex precursor", *Chem. Mater.*, **20**(5), 1688-1690.

CC